Hamedan University of Technology
Iranian Association of Electrical and Electronics Engineers

Sustainable Energy and Artificial Intelligence

Online ISSN: 3060-8015

Journal Homepage: www.enai.hut.ac.ir

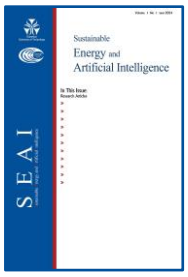

Location of Distributed Wind Energy with Consideration Capacity Credit Using the Monte-Carlo Method for Probabilities Evaluation of Wind

Mohammad Ali Arash[1], Mohammad Khakroei[1], Ashkan Mirzaei Rajeooni[2*]

[1] *MAPNA Electric & Control Engineering & Manufacturing Company (MECO), Alborz, Iran*
[2] *MAPNA Generator Engineering and Manufacturing Company (PARS), Alborz, Iran*
* *Corresponding Author: Mirzaei@mapnagenerator.com*

Article Info

Article type:
Original Article

Article history:
Received 2024-11-17;
Revised 2024-12-03;
Accepted 2024-12-08.

How to cite this article:
Arash, M., Khakroei, M. and Mirzaei Rajeooni, A. (2025). Location of Distributed Wind Energy with Consideration Capacity Credit Using the Monte-Carlo Method for Probabilities Evaluation of Wind. *Sustainable Energy and Artificial Intelligence*, *1*(1), 1-12. DOI: 10.61186/seai.2411-1022

Abstract

Significant advances have been made in electrical energy distribution networks in recent years. Distributed Generation (DG) technology is rapidly advancing, particularly in response to the needs of sensitive loads in the network that demand high reliability. This paper explores using distributed generation sources to increase capacity credit (CC) in Electrical energy distribution. This article focused on studying wind sources. The issue of planning DG in the distribution network is represented as a non-linear optimization problem. The goal is to make wind power more reliable, reduce losses, and improve capacity credit. The problem model includes the network's and DG's technical and economic constraints. Two methods, Monte Carlo and k-means, have been used to model uncertainties in network load and wind power generation during the planning process. The cut-set is used to assess the network's reliability. The IEEE 33-bus distribution network was studied using the teaching learning-based optimization algorithm in two scenarios to improve response efficiency. The article found that DG can provide up to 33% of the network load in capacity credit.

***Keywords*:** Capacity Credit, Distributed Generation, Generation Planning, Load Planning, Optimization Algorithm

1. Introduction

Research on distributed generation (DGs) and their role in distribution networks involves developing methods for planning DG sources while taking into account different goals and limitations. Proper planning is required for the integration of variable renewable energy sources into distribution networks to ensure reliable operation and achieve techno-economic goals such as reducing losses, enhancing reliability, increasing capacity credit, and so on. In most studies, distributed generation systems use a combination of energy sources for performance [1-4].

Some studies have looked into the network's capacity credit with wind turbines and battery-based energy storage. According to the articles, relying solely on wind turbines cannot improve reliability in the network, and using them excessively can decrease network reliability due to potential mismatches. Therefore, these articles suggest using a battery-based storage system alongside wind turbines. Also, the proposed system's capacity credit has been evaluated using effective load-carrying capacity (ELCC) [5-10]. However, increasing battery storage capacity will

be ineffective without expanding renewable generation capacity [11].

Some studies measure the capacity credit of solar cells and/or wind turbines for supplying the same generation capacity needed to meet the load [12]. A wind turbine provides better conditions than a solar cell. This is particularly important when the load peaks at night and solar power is at its lowest [6,13].

The impact of utilizing farms with high capacity on reliability and validity indicators has been a topic of discussion in numerous articles. Studies have shown that wind farms with larger generation capacities have higher validity in their capacity [7-9,14].

There are also articles available regarding demand response (DR) and its impact on the network's capacity credit. Studies have demonstrated that load response plans can enhance the system's capacity credit. Demand response not only alters the load profile but, also impacts the system's reliability. Therefore, implementing demand response can potentially modify the system's capacity credit. These references demonstrate that the utilization of DR can enhance the system's capacity credit when DG is present [15-17].

In a study conducted by [18], the authors focused on identifying optimal locations for capacitor banks to enhance voltage stability and minimize losses in distribution networks with scattered wind power generation. This reference highlights the impact of dispersed wind generation sources, which introduce uncertainty in output power. It suggests that power and voltage fluctuations are a direct result of this uncertainty, and proposes that the installation of capacitor banks can help improve network stability.

In [19], a discussion on the significance of reactive power compensation in the distribution network, VVVSN Murty et al. emphasized the integrated control of under load tap changer, dispersed sources, and distribution network consolidation for effective reactive power control.

In [20], using a Decomposition-based Multi-Objective Evolutionary algorithm (MOEA/D) improves 30-bus and 69-bus distribution networks by reducing Energy Not Supplied (ENS), which leads to reduced energy losses and voltage drop.It also shows that battery storage and distributed generation can improve grid reliability and reduce costs by reactive power compensation.

In [21], K Muthukumar et al. have highlighted the reduction in loss in distribution networks as the primary focus. They have implemented a triple response approach involving distributed generation sources, capacitor banks, and distribution network reorganization to achieve this goal.

In order to minimize losses in the electrical energy distribution network, [22] has located and planned solar and wind sources in the network. They have also utilized the particle swarm optimization (PSO) algorithm to effectively solve the optimization problem. Furthermore, research has also been carried out on the impact of economic conditions on the penetration of distribution networks and the restructuring of these networks [23-26]. It is shown in [27], although the three algorithms find almost similar optimal solutions, TLBO exhibits better convergence speed than PSO and Genetic Algorithm (GA).

Recent advancements in the development and improvement of wind turbine nominal capacity, such as Siemens Technology's 15 MW turbines, are leading to an increased utilization of this equipment in distribution networks. This article demonstrates that by strategically placing wind towers within the distribution network, significant enhancements in network capacity credit can be achieved. To achieve this goal, the first step is to frame the issue of planning wind DG as an optimization problem. The objective function is aimed at reducing losses, improving reliability, and increasing capacity credit. The cut set is instrumental in determining the system's reliability. The cut set relies on splitting the distribution network into two sections and assessing the reliability in each of these scenarios. The teaching-learning-based optimization (TLBO) algorithm will be utilized to address the optimization issue. This algorithm has the benefit of requiring only a few adjustable parameters while still maintaining a high level of accuracy and speed. A study was conducted on the IEEE 33-bus distribution network to demonstrate the effectiveness of the proposed response.

2. The Reliability of Distributed Generation and Teaching Algorithm

A system's reliability is determined by its capacity to execute designated tasks accurately and as scheduled within specific conditions over a given time frame. In this article, the reliability is calculated using the first-order cut-set.

In the TLBO algorithm, there is no visible separation between the teacher and the student. It is assumed that a group of individuals have assembled to acquire knowledge. Meanwhile, the individual with a greater understanding than the rest takes on the position of educator. Using this comparison, it makes sense to choose the student

who has the highest score in the subject to be the teacher, as they will strive to bring the rest of the class up to their level. Of course, it is unrealistic to expect all students in the class to achieve the same score as the teacher, as not every student will fully grasp the lesson. As a result, the class average is raised to a higher level than it was previously. Every time the iteration occurs, a student outperforms the teacher's score and replaces the teacher in the top spot, which is a continuous cycle. The training or teacher stage in the TLBO algorithm is commonly referred to as this process. Teaching in a class is not solely dependent on the teacher's efforts; students also have the opportunity to learn from one another. This collaborative learning process is known as the student stage. Fig. 1 shows the diagram of the TLBO algorithm [28].

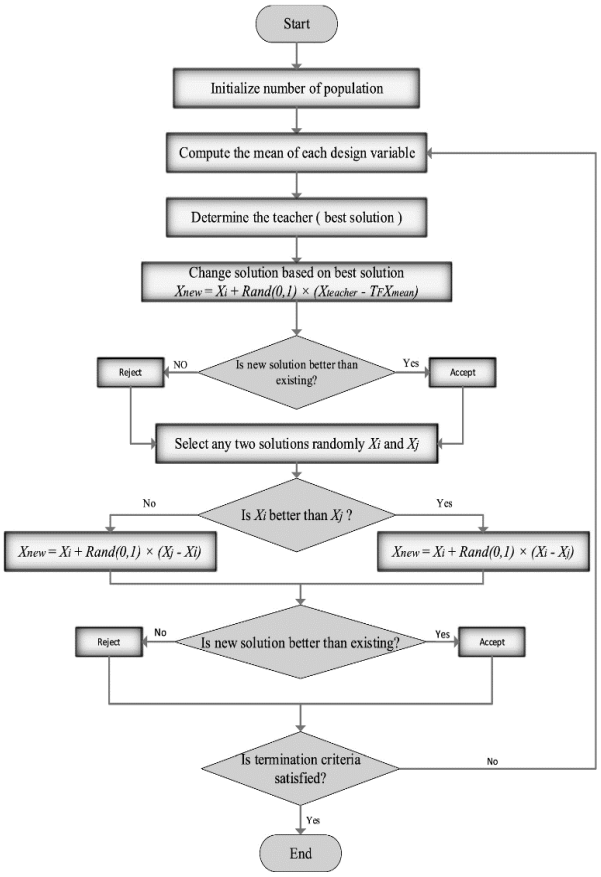

Fig. 1. Flowchart of the teaching-learning-based optimization (TLBO) algorithm [28]

2-1. Student Part

Two students, one with an X_j score and the other with a Xi score, are currently at different levels of knowledge. X_j wants to learn from Xi. The new score for the *j*th student can be expressed as a completely linear equation in this scenario. In the TLBO algorithm, the increase in a student j score is not modeled as a line. By using a random coefficient like rand, the training step becomes unpredictable. In this instance, it may be stated:

$$X_j^{new} = X_j + (X_j - X_i) \quad (1)$$

$$X_j^{new} = \begin{cases} X_j + rand \times (X_i - X_j) \ \ if \ \ X_i > X_j \\ X_j + rand \times (X_j - X_i) \ \ if \ \ X_j > X_i \end{cases} \quad (2)$$

j student's score will also show improvement if i student's score is higher than student j. Otherwise, student J actively avoids student *i* and diverts from their educational journey. Rand is a randomly generated number that falls within the range of 0 to 1 and follows a uniform distribution. The learning algorithm in the TLBO algorithm is often referred to as the student's algorithm [29].

2-2. Teacher Part

The T or X training program, also known as the teacher stage or training stage, helps move the average population and bring it closer to himself.

$$T = Teacher = M_{new}$$

$$X_i^{new} = X_i + \begin{Bmatrix} \vec{r}(Xj - Xi) \\ \vec{r}(Xi - Xj) \end{Bmatrix}$$

$$X_i^{new} = X_i + \vec{r}(M_{new} - TF \times M) \quad (3)$$

T: The best member of the crowd
X_i^{new}: New response
X_i: Old response
M: Current average
TF: Teaching factor

In this algorithm, the movement from M_{new} to M is applied to all members, which again adds a random value to M to improve the response [29].

3. Mathematical Model of the Proposed Algorithm

The references have indicated several ways to confirm the reliability of distributed generation systems, such as loss of load expectation (LOLE) and loss of energy expectation (LOEE) or expected energy not supplied (EENS). Additionally, factors like loss of power supply probability (LPSP), equivalent loss factor (ELF), and capacity credit (CC) are also important indicators. The above indicators are defined by the following equations [5]:

$$LOLE = \sum_{t=1}^{N} E[LOL(t)] \quad (4)$$

Equation (4) gives the mathematical representation of E [LOL (t)], the LOLE in the t time step. This can be further described using Equation (5).

$$E[LOL] = \sum_{s\in S} T_s \times P_s \quad (5)$$

The duration of load loss in case of being in the state of S is denoted by T_S, while P_S represents the probability of being in this state. S represents the full range of potential states that the system can exhibit.

$$LOEE = EENS = \sum_{t=1}^{N} E[LOE(t)] \quad (6)$$

Equation (6) defines E [LOE (t)] as the mathematical LOLE at the t interval, and this can be expressed using Equation (7).

$$E[LOE] = \sum_{s\in S} Q_s \times P_s \quad (7)$$

Q_S Represents the amount of load lost in state S, measured in kilowatt-hours. Equation (8) displays LPSP.

$$LPSP = \frac{LOEE}{\sum_{t=1}^{N} D(t)} \quad (8)$$

Equation (8) assumes that D (t) is equivalent to the load demand (kWh) at the t time step. Equation (9) provides a definition for ELF.

$$ELF = \frac{1}{N}\sum_{s\in S}\frac{Q(t)}{D(t)} \quad (9)$$

The CC focuses on assessing whether the current power system is able to meet the load demands in case some units are forced to shut down due to mechanical issues, weather changes, etc. This investigation is carried out under this specific topic. The CC is a measure of the power system's ability to withstand generation issues without compromising reliability. This capability can be examined from two perspectives: the enhancement of load capacity without compromising system reliability and the decrease in generation capacity with no impact on system reliability. CC is the defined capacity change. ELCC is the first case, while the second case is the force outage rate (FOR). The ELCC is computationally demonstrated by Equations (10) and (11). Also, Fig. 2 illustrates the Effective Load Carrying Capability concept [5].

$$LOLE = \sum_{i=1}^{N} E[Load + \sum \Delta L] \quad (10)$$

$$Capacity\ Credit = \frac{\sum \Delta L}{C} \quad (11)$$

Load changes are represented by ΔL, and C represents the capacity of the system. The load change is determined so that the LOLE remains constant. In this case, the CC of the system can be determined.

The researched distribution network consists of the IEEE 33-bus, which is linked to the upstream network via the first bus (as shown in Fig. 3) and feds from one end. In the peak state of the distribution network being studied, the total active load is 2300 kW and the total reactive load is 1800kvar. Table 1 indicates that the network voltage level is 12.66kV. Below, are explained these constraints [30].

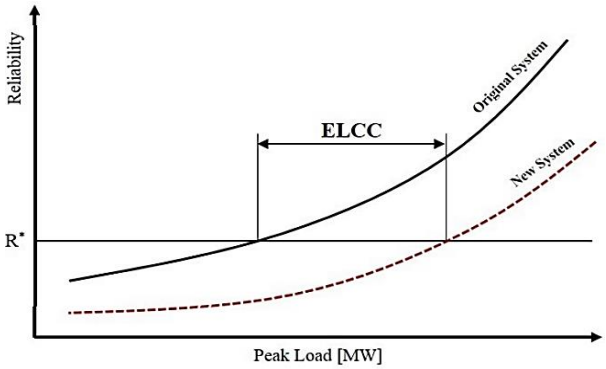

Fig. 2. Concept of effective load carrying capability [5]

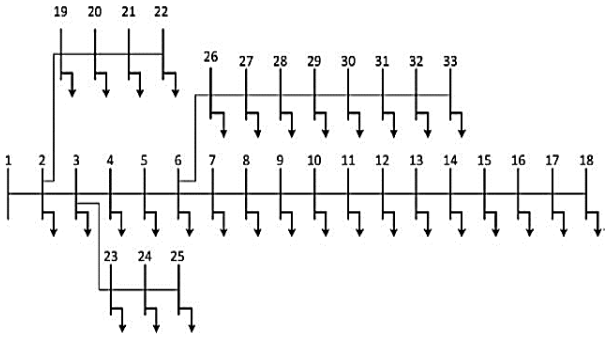

Fig. 3. IEEE 33-bus network

3-1. Active Power Distribution

Based on Equation (12), the power generated equals the aggregate of the total demand and loss. Here is an example of an equation that can be defined as [25,30]:

$$P_i(v,\delta) - P_{Gi} + P_{Di} = 0$$
$$P_i(v,\delta) = |V_i|\sum_{j=1}^{N}|V_j||Y_{ij}|\cos(\delta_i - \delta_j - \emptyset_{ij}) \quad (12)$$
$$Y_{ij} = |Y_{ij}|\angle\emptyset_{ij}$$

3-2. Reactive Power Distribution

As per Equation (13), the reactive power generated equals the combined total of demand and loss [25,30].

$$Q_i(v,\delta) - Q_{Gi} + Q_{Di} = 0$$
$$Q_i(v,\delta) = |V_i|\sum_{j=1}^{N}|V_j||Y_{ij}|\sin(\delta_i - \delta_j - \emptyset_{ij}) \quad (13)$$
$$Y_{ij} = |Y_{ij}|\angle\emptyset_{ij}$$

where L is loss, G is generation, and D is demand.

Table 1. Network data [30]

Sending bus	Receiving bus	R (Ohm)	X (ohm)	P_L (kW)	Q_L (kVAR)
1	2	0.0922	0.0470	100	60
2	3	0.4930	0.2511	90	40
3	4	0.3660	0.1864	120	80
4	5	0.3811	0.1941	60	30
5	6	0.8190	0.7070	60	20
6	7	0.1872	0.6188	200	100
7	8	0.7114	0.2351	200	100
8	9	1.0300	0.7400	60	20
9	10	1.0440	0.7400	60	20
10	11	0.1966	0.0650	45	30
11	12	0.3744	0.1238	60	35
12	13	1.4680	1.1550	60	35
13	14	0.5416	0.7129	120	80
14	15	0.5910	0.5260	60	10
15	16	0.7463	0.5450	60	20
16	17	1.2890	1.7210	60	20
17	18	0.7320	0.5740	90	40
18	19	0.1640	0.1565	90	40
19	20	1.5042	1.3554	90	40
20	21	0.4095	0.4784	90	40
21	22	0.7089	0.9373	90	40
22	23	0.4512	0.3083	90	50
23	24	0.8980	0.7091	420	200
24	25	0.8960	0.7011	420	200
25	26	0.2030	0.1034	60	25
26	27	0.2842	0.1447	60	25
27	28	1.0590	0.9337	60	20
28	29	0.8042	0.7006	120	70
29	30	0.5075	0.2585	200	600
30	31	0.9744	0.9630	150	70
31	32	0.3105	0.3619	210	100
32	33	0.3410	0.5302	60	40

3-3. Active and Reactive Power Balance in the Network

The standard specifies that the maximum active power allowed is 2300kW, while the maximum reactive power permitted is 1800kVar. Based on the information provided, the total generation with loss and use equals zero [25,30].

$$\begin{cases} \sum_{i=1}^{N_G} P_{L_i} - \sum_{i=1}^{N_D} P_{D_i} - P_L = 0 \\ \sum_{i=1}^{N_G} Q_{L_i} - \sum_{i=1}^{N_D} Q_{D_i} - Q_L = 0 \end{cases} \quad (14)$$

3-4. Bus Voltage

The network voltage is 12.66kV, with V_i representing the bus i voltage. V_{min} and V_{max} refer to the lowest and highest voltage ranges of the bus. Therefore, the maximum voltage passing through feeder j is restricted to V_{max} [1,25].

$$V_{min} \le V_i \le V_{max} \quad (15)$$

3-5. Occupied Capacity of the Feeder

A set of 33 buses in the secondary has a maximum thermal capacity of 16, while in the primary feeders, it is 6.6 megavolt amps. Therefore, the maximum power that can pass through feeder j is F_{max}.

$$|F_j| \le F_{max} \quad (16)$$

3-6. Maximum Number of Distributed Sources in Each Bus of the Micro-Network

Where the total number of dispersed sources used in the network, N_{dg}, is limited to $N_{dg\,max}$.

$$N_{DG} \le N_{dgmax} \quad (17)$$

3-7. Maximum Capacity of Dispersed Generation Source

Therefore, the maximum capacity of distributed sources in the distribution network is restricted to C_{dgmax}.

$$C_{dg} \le C_{dgmax} \quad (18)$$

Equation (19) represents the objective function. This term consists of three goals. The primary goal is to decrease ENS within the network. The ENS refers to the load on the shared side that is unable to receive power due to outages and malfunctions in the power system. The second goal is to minimize losses within the distribution network. The third objective function represents the cost of scattered wind power sources [31].

$$Min\ F = C_1 \sum_{i=1}^{N_{bus}} ENS_i + C_2 \sum_{j=1}^{N_{branch}} R_j \times |I|^2 - C_3 \times ELCC \quad (19)$$

To maintain the highest reliability of the distribution network while incorporating DG, the CC is determined as the maximum load increase possible without compromising network reliability. The function is defined in a way that minimizes the network ENS and loss, and maximizes the CC. This decision is made to reach the maximum potential of the CC. As per the above statement, the loss and ENS are denoted with a positive sign in the formula of the objective function, while the value of the CC is denoted with a negative sign.

4. Confirmation of Capacity Credit of Wind Sources in the Distribution Network

The CC of DG in the distribution network is the

maximum load that can be integrated with the existing base load without compromising the reliability of the network when dispersed wind generation sources are added. This ensures that the network remains reliable even with the addition of wind sources, in comparison to the primary network. Fig. 4 displays the verification of the CC for distributed wind generation sources within the distribution network. First, the distribution network is simulated for this purpose, followed by modeling the uncertainty of wind sources and network load based on the described method. Second, the reliability index of the distribution network is determined without taking into account wind sources but rather focusing solely on the uncertainties related to the network load. In the next stage, the reliability index of the distribution network is then assessed by considering the uncertainties arising from dispersed wind generation sources. As per the CC's definition of wind sources, the distribution network load is incrementally increased to assess the impact on reliability. The reliability index is then compared between scenarios with and without wind sources at each step of increased network load.

An increase in network load was reported, with the network reliability index remaining the same when wind sources and the primary network, were both present. The ENS of the network serves as the reliability index discussed in this article, and its verification process is explained in the following section.

5. Modeling and Problem - Solving

5-1. Modeling the Output Power of Wind Turbines

The hourly power output of the wind turbine can be determined by analyzing the average wind speed at the turbine tower's height and the specific features of the turbine. Hence, it is essential to first determine the average wind velocity at the height of the wind turbine tower before proceeding to calculate its output power. Equation (20) can be used to calculate the wind speed at any given height by utilizing the wind speed measured at a certain height [2].

$$\frac{V_1}{V_2} = (\frac{h_2}{h_1})^{\alpha} \tag{20}$$

The parameter v_2 in Equation (20) represents the wind velocity at height h_2, while v_1 is the velocity measured at the reference height h1. In this article, the coefficient of friction α is considered with the value of 25. The Weibull probability distribution function is employed to represent the variability resulting from changes in wind speed. The wind speed is calculated and once that is done, Equation (21) can be used to determine the output power of the wind generator [1,2].

$$P_{WT}: \begin{cases} 0 & V < V_{cut-in}, V > V_{cut-in} \\ V^3 \left(\frac{P_r}{V_r^3 - V_{cut-in}^3}\right) - P_r \left(\frac{V_{cut-in}^3}{V_r^3 - V_{cut-in}^3}\right) & V_{cut-in} \le V \\ P_r & V_{rated} \le V < V_{cut-in} \end{cases} \tag{21}$$

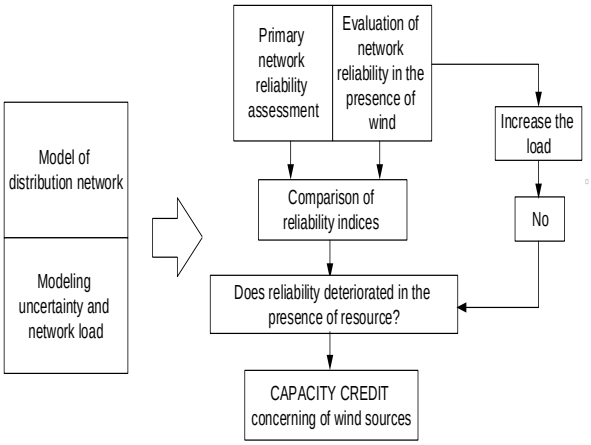

Fig. 4. Process of confirming capacity credit of dispersed wind generation sources

The wind speed per hour is represented by V in Equation (21), while P_r represents the rated power of the generator. The connection velocity, rated velocity, and cut-off velocity of the wind turbine are V_{cut-in}, V_{rated}, and $V_{cut-out}$, respectively. The output power diagram of a typical wind turbine is shown in Fig. 5.

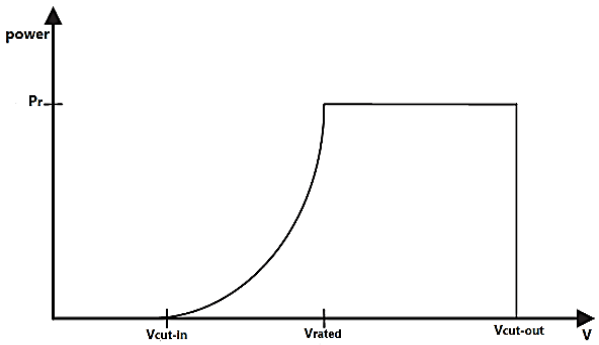

Fig. 5. Process of confirming capacity credit of dispersed wind generation sources

5-2. Load Modeling

Modeling the uncertainty of the network load

involves using a probabilistic method that relies on the normal distribution function. The mean value is 100% while the standard deviation is 10%.

5-3. Studied Network

The IEEE 33-bus network has been analyzed, featuring a total load of 2300kW active and 1800kVAR reactive power being supplied from one direction. The network operates at a voltage level of 12.66kV, with detailed specifications available in Table 2. Additionally, Fig. 3 displays the single-line diagram for the network.

5-3-1. Initial Evaluation of the Network

Fig. 6 displays the voltage curve in order to assess the distribution network, while Fig. 7 illustrates the power profile for each feeder.

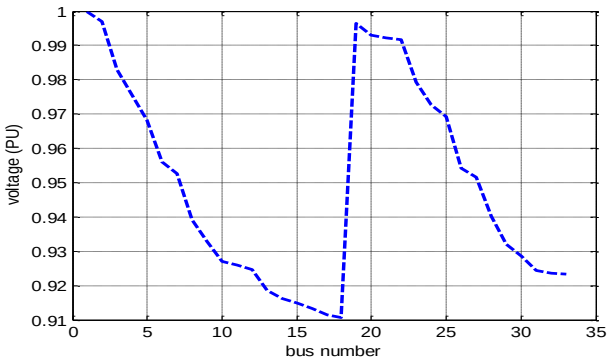

Fig. 6. Voltage curve of the studied distribution network

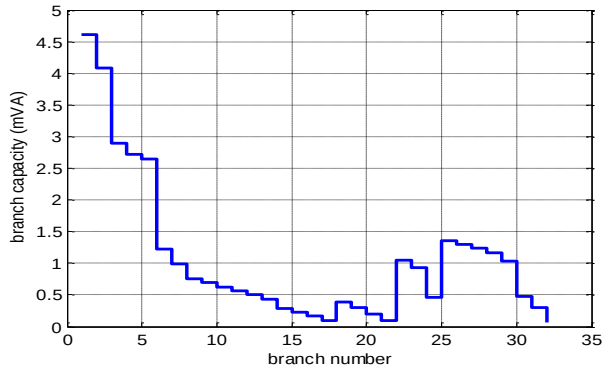

Fig. 7. Voltage curve of the studied distribution network

Table 2 outlines the specific segmentation of the network into smaller components. Each segment is equipped with different equipment from Table 3 and has specific load characteristics outlined in Table 4. Table 5 provides information on the probability of equipment failure and the corresponding rates for repairs.

Table 2. Segmentation of the studied network

Unit No.	Bus bars related to the unit
1	22-21-20-19
2	1 to 18
3	25-24-23
4	26 to 33

Table 3. Information of equipment connected to each part

Section No.	Components of the first section	Components of the second section
1	2 bus bars (bus 1-2) 1 Circuit breaker 2 cables (the cable connecting the substation to bus bar no 1 and the cable connecting bus bar (1) & bus bar (2)	1 Circuit breaker 1 Cable (cable at the beginning of the line) 1 Bus bar (bus bar at the beginning of the line)
2	1 Cable (cable connecting substation and first bus bar) Circuit breaker Substation	1 Circuit breaker 1 Cable (cable at the beginning of the line) 1 Bus bar (bus bar at the beginning of the line)
3	3 bus bars (buses one, two and three) four cables (cables connecting the substation and the first bus, the first bus to the second bus, the second bus to the third and the third bus to the twenty-third bus) the circuit breaker of the Substation	1 Circuit breaker 1 Cable (cable at the beginning of the line) 1 Bus bar (bus bar at the beginning of the line)
4	6 bus bars (first to sixth bus bars) 7 cables (cables from the Substation to the 26th bus) circuit breaker substations	1 Circuit breaker 1 Cable (cable at the beginning of the line) 1 Bus bar (bus bar at the beginning of the line)

Table 4. Information of equipments connected to each section

Section No.	The number of consumers in each section	Load consumption (MW)
1	800	36
2	3000	605.1
3	600	93
4	1500	92

Table 5. Failure rate and repair time of system components

Repair Rates	Failure Rates%	Equipment
10	0.002	Circuit breaker
10	0.05	bus bar
10	0.06	Cable
10	0.001	Substation

5-3-2. Uncertainty Modeling

This article considers two uncertainties. There are two main uncertainties associated with wind turbines: the uncertainty of the load and the uncertainty of the output power.

The wind speed uncertainty has been modeled using the Weibull distribution function, with shape and scale parameters set at 2 and 7, respectively [32]. The normal distribution function changes the network load by adjusting the mean and standard deviation to 100% and 10%, respectively. Finally, The Monte Carlo method is used to take 1000 samples from each probability distribution function. Next, the data matrix is created and the k-means method is utilized to simplify the scenario. The wind turbine was deemed to have a nominal capacity of 1 MW. The results of this modeling are shown in Table 6. This article examines two ways to plan dispersed wind generation sources. The first method: According to ENS, the discussion in this section focuses on planning dispersed wind generation sources to decrease loss and enhance reliability. All the considerations mentioned above have been taken into account for the o$_{pt}$imization process. Additionally, the settings of the TLBO algorithm have been implemented in the algorithm.

Table 6. Results of modeling the uncertainties of wind sources and load

load	Wind turbine output power (1MW)	Possibility
0.999938679	0.680968731	0.157
1.000851845	0.237879369	0.228
1.001851094	0.025804531	0.272
0.992901941	0.445224207	0.217
0.9915612	0.957973492	0.126

Fig. 8 displays the objective function's enhancement process. In Table 7, the optimal response, location, and capacity for installing distributed sources are displayed. Fig. 8 shows a notable decrease in the value of the objective function. Table 8 displays the network's loss and ENS values in both optimal and normal states, along with the objective function sentences. ENS reported an increase in the network's reliability of 42% and a 40% decrease in network loss.

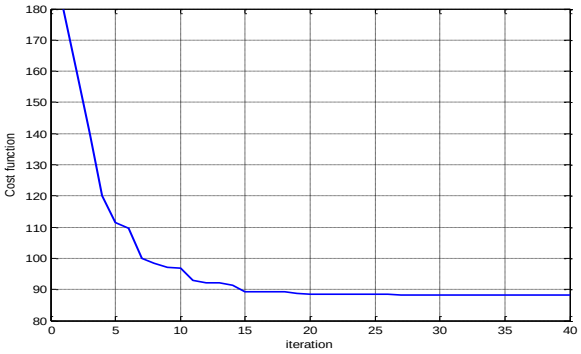

Fig. 8. Improvement process of the objective function

Table 7. Styles Optimum location and capacity for installing distributed wind generation sources

location	Wind turbine output power (1MW)
21	0.391569999
8	1.572508512
24	0.975649865
30	0.960358298

Table 8. Comparison of network performance in optimum and normal states

Description	normal	optimum
Annual energy loss (MWh)	1826	1162
Amount of unsupplied annual energy (MWh)	1.49E+6	0.88+E6

Fig. 9 displays the bus voltage, while Fig. 10 depicts the power passing through the distribution network feeders in both the optimum and normal states when considering uncertainty modeling in scenario 1. The network bus voltage curve indicates a better network bus voltage than the standard state. Additionally, there has been a notable decrease in the amount of power flowing through the network feeders. DG in the distribution network allows for power to be supplied directly to the point of consumption, reducing the need to inject power into the network from upstream. In addition, voltage drop has been minimized, leading to a reduced voltage deviation of the network's buses from the standard value.

Second method: The planning of wind sources in the distribution network is being discussed to enhance the CC of dispersed wind generation sources. As outlined in section (5), the uncertainty of wind sources and network load is modeled in a closed loop to assess the reliability of the distribution network as the base load continues to rise. The comparison is made between the distribution network's reliability with and without the presence of wind sources. The objective function was confirmed as equalizing the reliability of the network in two states when the load increase occurred. The TLBO algorithm was used to reduce

capacity credit, thus maximizing it.

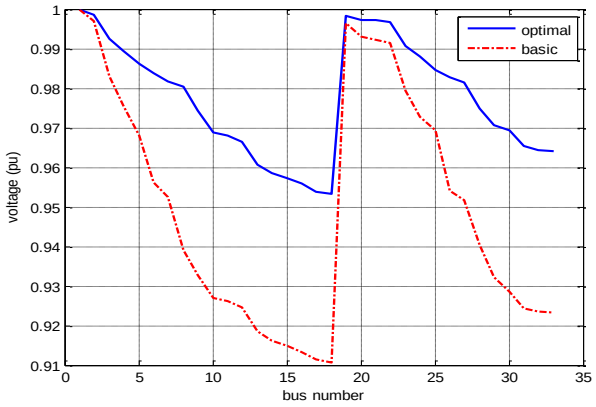

Fig. 9. Improvement process of the objective function

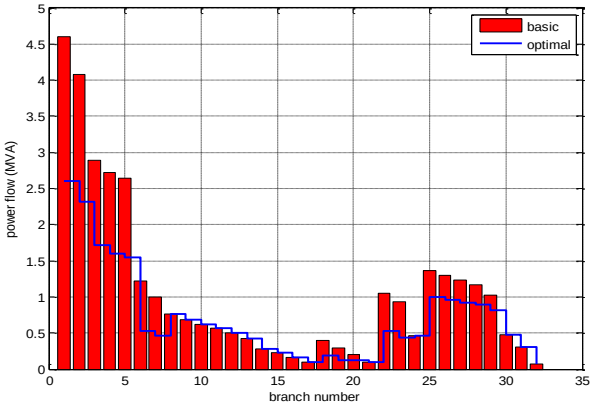

Fig. 10. Power profile of the feeders of the distribution network in the first case of 5 uncertainties

Fig. 11 illustrates the progress of the objective function enhancement. Table 9 displays the optimal installation location and capacity for distributed wind generation sources in the distribution network, with a calculated CC of 0.33 compared to the base network value of 3.34. Table 10 illustrates the comparison between the distribution network's performance in the optimum state under scenario 2 and its performance in the normal state. The distribution network's performance has improved significantly under this scenario where the goal was to maximize the CC of the dispersed wind generation sources. This improvement is evident in the reduction of initial state losses. Nevertheless, the goal of this scenario did not include reducing losses. While the main goal of this situation was to increase the CC of dispersed wind generation sources, there has been a notable enhancement in reliability with the integration of wind sources, as indicated by ENS. Fig. 12 and Fig. 13 display the bus voltage and power flowing through the distribution network feeders in both optimal and normal conditions for the initial state of the five potential states used to simulate uncertainties. The utilization of the distribution network with DG present appears to be optimal, even when planned with the objective of enhancing the CC.

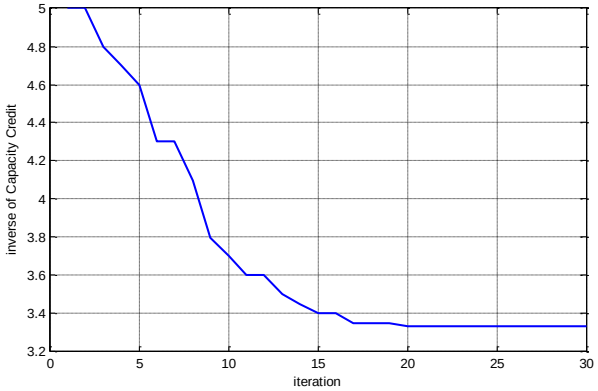

Fig. 11. Process of improving the objective function under method 2

Table 9. Optimum location and capacity for installing distributed wind generation sources

Location	Wind turbine output power (1MW)
20	1.1
18	0
23	1.2847
26	1.3322

Table 10. Comparison of the network performance in optimum and normal states under the second scenario

Network performance	Normal	Optimum
Annual energy loss (MWh)	1826	1715
Amount of unsupplied annual energy (MWh)	1.49E+06	3.53E+05

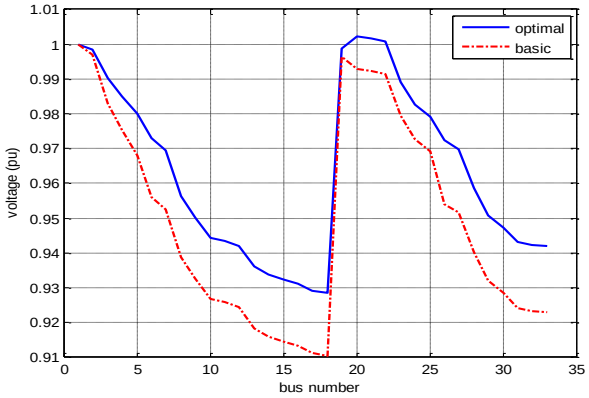

Fig. 12. Voltage curve of distribution network buses in optimum and normal states in the first state of 5 uncertainty modes

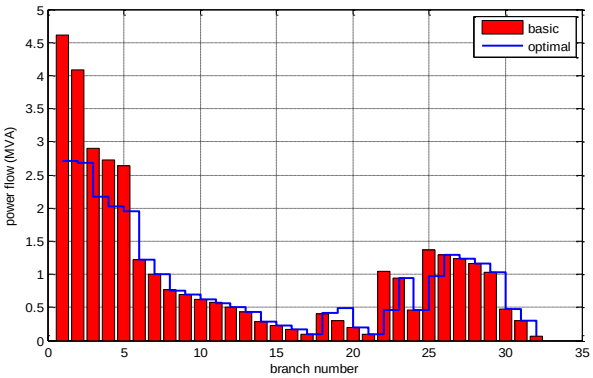

Fig. 13. Power profile of the feeders of the distribution network in the third state of the 5 uncertainty states

6. Conclusion

The TLBO algorithm is implemented in this study to obtain the desired outcome. This algorithm makes it easier to find the answer by using fewer parameters compared to other algorithms, along with two extra parameters for exploitation and exploration. Using the TLBO algorithm, an attempt was made to plan distributed generation sources in the distribution network with respect to capacity credit.

ENS has reported an increase of about 40% in the reliability of capacity credit when dispersed wind generation sources are present in the distribution network. Capacity credit was calculated by accessing the initial sources and then considering ELCC as one of the main parameters related to reliability in the network. The study found that distributed wind generation sources in the distribution network have a capacity credit of 33% of the base load, showing their significant contribution. This article demonstrates that incorporating dispersion of wind generation sources in the distribution network, without the addition of storage sources like solar cells, plays a crucial role in enhancing the network's reliability and boosting its CC.

References

[1] Khasanov, M., Kamel, S., Rahmann, C., Hasanien, H. M., & Al-Durra, A. (2021). Optimal distributed generation and battery energy storage units integration in distribution systems considering power generation uncertainty. *IET Generation, Transmission & Distribution*, *15*(24), 3400-3422.

[2] Zarate-Perez, E., Santos-Mejía, C., & Sebastián, R. (2023). Reliability of autonomous solar-wind microgrids with battery energy storage system applied in the residential sector. *Energy Reports*, *9*, 172-183.

[3] Naderipour, A., Kamyab, H., Klemeš, J. J., Ebrahimi, R., Chelliapan, S., Nowdeh, S. A., ... & Marzbali, M. H. (2022). Optimal design of hybrid grid-connected photovoltaic/wind/battery sustainable energy system improving reliability, cost and emission. *Energy*, *257*, 124679.

[4] Hassan, Q., Algburi, S., Sameen, A. Z., Salman, H. M., & Jaszczur, M. (2023). A review of hybrid renewable energy systems: Solar and wind-powered solutions: Challenges, opportunities, and policy implications. *Results in Engineering*, 101621.

[5] Oh, U., Choi, J., & Kim, H. H. (2016, October). Capacity credit and reasonable ESS evaluation of power system including WTGs combined with BESS. In *2016 International Conference on Probabilistic Methods Applied to Power Systems (PMAPS)* (pp. 1-6). IEEE.

[6] Hu, L., Jun, H., Junhui, H., Linwei, Z., Hong, L., Zhe, W., & Hongda, Z. (2016, August). Capacity credit evaluation of distributed generations and analysis of its influence factors. In *2016 China International Conference on Electricity Distribution (CICED)* (pp. 1-5). IEEE.

[7] de Guzman, A. J. R., & Tio, A. E. D. (2016, June). Capacity credit of Philippine wind farms in Luzon. In *2016 IEEE 16th International Conference on Environment and Electrical Engineering (EEEIC)* (pp. 1-5). IEEE.

[8] Sallam, A., El-Khattam, W., & El-Salmawy, H. (2016, December). Economic impact of Capacity Credit evaluation for Wind Energy Conversion Systems projects in Egypt. In *2016 Eighteenth International Middle East Power Systems Conference (MEPCON)* (pp. 664-669). IEEE.

[9] Tómasson, E., & Söder, L. (2017, December). Multi-area generation adequacy and capacity credit in power system analysis. In *2017 IEEE Innovative Smart Grid Technologies-Asia (ISGT-Asia)* (pp. 1-6). IEEE.

[10] Jiahao, C., Bing, S., Yuan, Z., Ruipeng, J., Yunfei, L., & Shiqian, M. (2023). A united credible capacity evaluation method of distributed generation and energy storage based on active island operation. *Frontiers in Energy Research*, *10*, 1043229.

[11] Gangopadhyay, A., Seshadri, A. K., & Patil, B. (2024). Wind-solar-storage trade-offs in a decarbonizing electricity system. *Applied Energy*, *353*, 121994.

[12] Amarasinghe, P. A. G. M., & Abeygunawardane, S. K. (2019, July). Capacity credit evaluation of wind and solar power generation using non-sequential Monte Carlo Simulation. In *2019 Moratuwa Engineering Research Conference (MERCon)* (pp. 205-210). IEEE.

[13] Freeman, S., & Agar, E. (2024). The impact of energy storage on the reliability of wind and solar power in New England. *Heliyon*, *10*(6).

[14] Sulaeman, S., Benidris, M., Tian, Y., & Mitra, J. (2016, May). Modeling and evaluating the capacity credit of PV solar systems using an analytical method. In *2016 IEEE/PES Transmission and*

Distribution Conference and Exposition (T&D) (pp. 1-5). IEEE.

[15] Feng, J., Zeng, B., Zhao, D., Wu, G., Liu, Z., & Zhang, J. (2017). Evaluating demand response impacts on capacity credit of renewable distributed generation in smart distribution systems. *IEEE Access*, *6*, 14307-14317.

[16] Parks, K. (2019). Declining capacity credit for energy storage and demand response with increased penetration. *IEEE Transactions on Power Systems*, *34*(6), 4542-4546.

[17] Zeng, B., & Wei, X. (2018, September). Capacity credit assessment of demand response based on a rigorous uncertainty modeling framework. In *2018 IEEE Industry Applications Society Annual Meeting (IAS)* (pp. 1-8). IEEE.

[18] Ramadan, H. S., Bendary, A. F., & Nagy, S. (2017). Particle swarm optimization algorithm for capacitor allocation problem in distribution systems with wind turbine generators. *International Journal of Electrical Power & Energy Systems*, *84*, 143-152.

[19] Murty, V. V. V. S. N., & Sharma, A. K. (2019). Optimal coordinate control of OLTC, DG, D-STATCOM, and reconfiguration in distribution system for voltage control and loss minimization. *International Transactions on Electrical Energy Systems*, *29*(3), e2752.

[20] Hamidan, M. A., & Borousan, F. (2022). Optimal planning of distributed generation and battery energy storage systems simultaneously in distribution networks for loss reduction and reliability improvement. *Journal of Energy Storage*, *46*, 103844.

[21] Muthukumar, K., & Jayalalitha, S. J. A. S. C. (2017). Integrated approach of network reconfiguration with distributed generation and shunt capacitors placement for power loss minimization in radial distribution networks. *Applied Soft Computing*, *52*, 1262-1284.

[22] Naeem, A., Hassan, N. U., & Yuen, C. (2018, May). Power loss minimization in power distribution systems using wind and solar complementarity. In *2018 IEEE Innovative Smart Grid Technologies-Asia (ISGT Asia)* (pp. 1165-1170). IEEE.

[23] Ismael, S. M., Aleem, S. H. A., Abdelaziz, A. Y., & Zobaa, A. F. (2019). State-of-the-art of hosting capacity in modern power systems with distributed generation. *Renewable energy*, *130*, 1002-1020.

[24] Takenobu, Y., Yasuda, N., Minato, S. I., & Hayashi, Y. (2019). Scalable enumeration approach for maximizing hosting capacity of distributed generation. *International Journal of Electrical Power & Energy Systems*, *105*, 867-876.

[25] Koutsoukis, N. C., Siagkas, D. O., Georgilakis, P. S., & Hatziargyriou, N. D. (2016). Online reconfiguration of active distribution networks for maximum integration of distributed generation. *IEEE Transactions on Automation Science and Engineering*, *14*(2), 437-448.

[26] Esmaeili, S., Anvari-Moghaddam, A., Jadid, S., & Guerrero, J. M. (2019). Optimal simultaneous day-ahead scheduling and hourly reconfiguration of distribution systems considering responsive loads. *International Journal of Electrical Power & Energy Systems*, *104*, 537-548.

[27] Toopshekan, A., Abedian, A., Azizi, A., Ahmadi, E., & Rad, M. A. V. (2023). Optimization of a CHP system using a forecasting dispatch and teaching-learning-based optimization algorithm. *Energy*, *285*, 128671.

[28] Dastan, M., Shojaee, S., Hamzehei-Javaran, S., & Goodarzimehr, V. (2022). Hybrid teaching–learning-based optimization for solving engineering and mathematical problems. *Journal of the Brazilian Society of Mechanical Sciences and Engineering*, *44*(9), 431.

[29] Alizadeh, E., Maleki, A., & Amirara, H. (2017). Modified Teaching Learning Based Optimization. In *Congress of Interdisciplinary Studies in Science and Engineering*.

[30] Ukut, U. I., Okpura, N., & Tim, P. O. The IEEE 33 Bus Distribution System Load Flow Analysis Using Newton Raphson Method.

[31] Chen, F., Li, F., Feng, W., Wei, Z., Cui, H., & Liu, H. (2019). Reliability assessment method of composite power system with wind farms and its application in capacity credit evaluation of wind farms. *Electric Power Systems Research*, *166*, 73-82.

[32] Delbari, M., Kahkha Moghaddam, P., Mohammadi, E., & Ahmadi, T. (2016). Estimation of the spatial distribution pattern of wind speed for assessment of wind energy potential in Iran. *Physical Geography Research Quarterly*, *48*(2), 265-285.

Biography

Mohammad Ali Arash graduated from Islamic Azad University, South Tehran Branch, in 2004 and 2023 with a B.Sc. and M.Sc. degrees in electrical engineering. In 2007, he joined the Tehran branch of TEXTAR Company for two years, and then joined Mapna Electric & Control Engineering & Manufacturing. He works in a very friendly engineering team that works on SEE, SFC, and VFDs of various types. His research interests include optimization algorithms such as TLBO, Genetics, Harmonic analysis, mathematical and physics, transformers, and power electronics.

Mohammad Khakroei obtained his B.Sc. and M.Sc. degrees in electrical engineering from Shahid Beheshti University and Iran University of Science and Technology in 2015 and 2019, respectively. In 2022, he joined MAPNA Electric & Control Engineering & Manufacturing Company (MECO), Alborz, Iran as an expert within the engineering team specializing in SEE, SFC, and VFD. His research interests include numerical modeling of electrical equipment using the Finite Element Method (FEM), transformers, and power electronics.

Ashkan Mirzaei Rajeooni received his B.Sc. degree in electrical engineering in 2016 and his M.Sc. degree in electrical engineering from Iran University of Science and Technology in 2019. Currently, he is working as an Electrical expert at the Department of Engineering and R&D of MAPNA Generator Engineering and Manufacturing Company (PARS), Alborz, Iran. His research interests include numerical modeling of electrical equipment using the Finite Element Method (FEM), transformers, bus ducts, and fault current limiters.